Received: 11 October 2018 | Accepted: 27 March 2019

DOI: 10.1002/hyp.13459

DATA NOTE

WILEY HP TODAY

Towards estimating root-zone soil moisture using surface multispectral and thermal sensing: A spectral and hydrometeorological dataset from the Dookie experiment site, Victoria, Australia

Venkata Radha Akuraju[1,2] | Dongryeol Ryu[1] | Andrew William Western[1] | Rodger Ian Young[1]

[1] Department of Infrastructure Engineering, The University of Melbourne, Parkville, Victoria, Australia

[2] ICRISAT Development Centre, International Crops Research Institute for the Semi-Arid Tropics, Patancheru, Hyderabad, India

Correspondence
Venkata Radha Akuraju, Department of Infrastructure Engineering, The University of Melbourne, Parkville, Victoria 3010, Australia.
Email: avenkataradha@gmail.com

Funding information
Australian Centre for International Agricultural Research, Grant/Award Number: JAF; The Australian Research Council, Grant/Award Number: LE130100040

Abstract

This paper describes surface hydrometeorological and spectral datasets collected from two tower sites located in the University of Melbourne's Dookie experimental farm, Victoria, Australia. The datasets were collected from different vegetation types including wheat, canola, and grazed pasture during the 2012, 2013, and 2014 cropping seasons. The dataset includes 30-min frequency latent and sensible heat flux measurements and layer-average soil moisture data at profile depths of 0–5, 0–30, 30–60, 60–90, and 90–120 cm. Air temperature, wind speed, wind direction, relative humidity, precipitation, and incoming and outgoing longwave and shortwave radiation data were also collected from two locations in the study area. The dataset described in this paper is available online.

1 | SITE DESCRIPTION AND METHODS

The Dookie hydrometeorological and spectral dataset was collected at the Dookie agriculture farm, operated by the University of Melbourne, Victoria, Australia. The climate is Mediterranean semiarid with hot/dry summers and cold/wet winters (Bell, Eckard, & Cullen, 2012). The study sites are located in the south-west part of the Murray-Darling Basin and used for rain-fed agriculture (Figure 1). Two meteorological towers were installed in the study area. Study Site 1 was lucerne (*Medicago sativa*) pasture land used for sheep grazing in 2012 and covered with grass pasture in 2013. Wheat (*Triticum aestivum*) crops were grown at Study Site 2 in 2012 and 2013. In 2014, canola (*Brassica napus*) was grown at both study sites.

The key hydrometeorological and spectral dataset consists of meteorological, soil hydrological, and spectral (multispectral and thermal infrared bands) data. A time-series meteorological and soil hydrological dataset was collected in 30-min intervals, and a spectral dataset was collected in 5-min intervals. Data were collected continuously from January 01, 2012, to December 31, 2014, at Study Site 1 and from August 15, 2012, to December 31, 2014, at Study Site 2. Meteorological data, which include air temperature, wind speed, relative humidity, atmospheric pressure, incoming and outgoing longwave and shortwave radiations, and rainfall, were collected continuously from January 01, 2012, to December 31, 2014, at both sites. Flux data were collected continuously during 2012 and 2013 but only for the cropping period in 2014. Actual sowing and harvesting dates are provided in Table 1.

Soil hydrological data composed of soil moisture measurements at 0–5, 0–30, 30–60, 60–90, and 90–120 cm and soil profile temperatures at 10, 20, 50, and 95 cm. Spectral data at both study sites consisted of surface reflectance data corresponding to relevant Landsat and MODIS (Moderate Resolution Imaging Spectroradiometer) spectral bands, and radiative surface temperature. Spectral data can be used to monitor crop phenology and calculate vegetation indices such as the normalized difference vegetation index (NDVI), the photochemical reflectance index, and the crop water stress index. In addition to spectral data, vegetation height was measured during our frequent visits to the study sites. Cameras were installed at both study sites to monitor vegetation cover and sheep grazing activities.

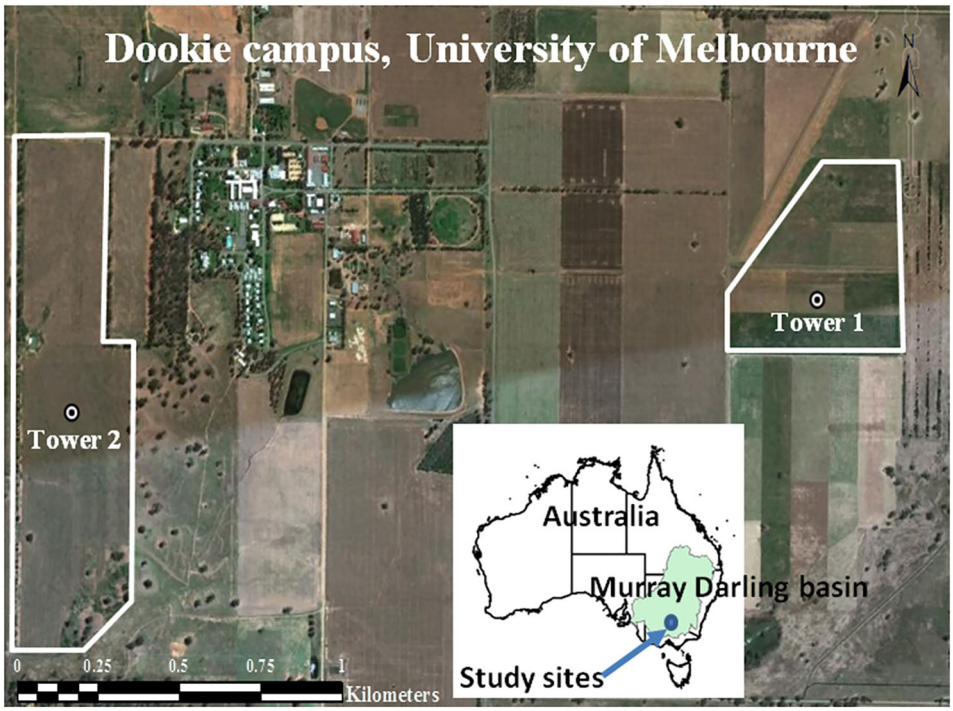

FIGURE 1 Location of Dookie experimental farm and study sites

All sensors were connected to CR3000 and CR5000 data loggers (Campbell Scientific, Inc.) for data storage. Field visits were planned approximately twice a month in order to download data. Although all sensors collected data automatically, periodic level checks, levelling adjustments, and cleaning were undertaken to maintain accuracy of data collection. Field visit days and activity log file have been added to the online data repository.

2 | METEROLOGICAL DATASET

Meteorological data consisting of air temperature, wind speed and direction, relative humidity, atmospheric pressure, net radiation, rainfall, latent heat flux, sensible heat flux, and soil heat fluxes were collected at both study sites. Wind speed and wind direction were measured using a wind sentry set (03101 R.M. Young) that consisted of a three-cup anemometer and a potentiometer. Air temperature and relative humidity were measured using an HMP45C probe (Campbell Scientific, Inc.). A CS105 barometric pressure sensor (Campbell Scientific, Inc.) equipped with Vaisala's capacitive pressure sensor was used to measure barometric pressure. The output of the sensor in the form of current ranges from 0 to 2.5 V that corresponds to pressure from 600 to 1,060 mb. All meteorological measurements were collected available at 30-min intervals.

TABLE 1 Crop type, sowing, and harvesting dates for each site and year

Site name	Year	Vegetation type	Sowing date	Harvesting date
Study Site 1	2012	Lucerne	NA	NA
	2013	Pasture	NA	NA
	2014	Canola	Apr 23	Nov 10
Study Site 2	2012	Wheat	May 15	Dec 07
	2013	Wheat	May 24	Dec 17
	2014	Canola	Apr 24	Nov 10

Abbreviation: NA, not applicable.

2.1 | Net radiation

A CNR1 net radiometer (Kipp & Zonen, Inc.) was used to measure the upwards and downwards shortwave and longwave radiation components. Sensor output (V) was converted to radiative flux (W/m^2) using manufacturer-supplied calibration coefficients. Net radiation was calculated as follows:

$$R_n = R_{s\downarrow} + R_{L\downarrow} - R_{S\uparrow} - R_{L\uparrow}. \quad (1)$$

The subscripts S and L represent shortwave and longwave radiation, respectively, and upward and downward arrows represent incoming and outgoing radiation. Daily net radiation for 2013 is shown in Figure 2b.

2.2 | Rainfall

The TR-525 rainfall sensor (Texas Electronics, Inc.), a tipping bucket rain gauge (0.2-mm tip size), was installed at a height of 1 m at both study sites in order to measure rainfall. Cumulative rainfall was recorded over a 30-min interval. A collecting rain gauge was installed at study sites to measure the total rainfall between bimonthly

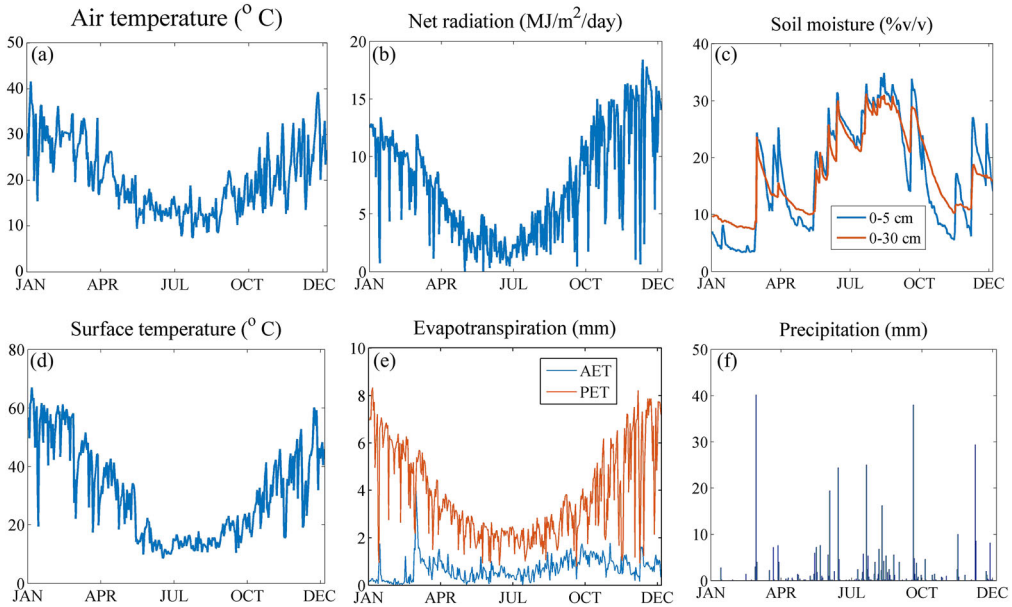

FIGURE 2 Example daily time series from Study Site 2 for 2013. (a) Daily maximum air temperature, (b) daily net radiation, (c) volumetric soil moisture at 0–5 and 0–30 cm, (d) daily maximum radiative surface temperature, (e) daily actual and Priestley–Taylor potential evapotranspiration, and (f) daily rainfall

maintenance visits and was compared with tipping bucket rain gauge measurements.

2.3 | Flux measurements

Latent and sensible heat fluxes were measured using the eddy covariance method. The eddy covariance system consisted of an LI-7500 open path gas analyser (LI-COR, Inc.) and CSAT3 three-dimensional sonic anemometer (Campbell Scientific, Inc.) connected to a CR5000 data logger (Figure 3). Turbulent fluctuation measurements of three-dimensional velocity, humidity, and sonic temperature were recorded at a frequency of 20 Hz for post-processing. The Eddy-Pro software (LI-COR, Inc.) was used to correct high-frequency data and for quality control. A metadata file was configured with instrument height, direction, sensor separation, and dynamic canopy height from field observations. Flux data were corrected to reduce the effects of density fluctuations due to humidity and temperature fluctuations, and default spectral corrections applied (Moncrieff et al., 1997; Webb, Pearman, & Leuning, 1980). The high-frequency 20-Hz eddy covariance data can be shared upon request; however, the high-frequency dataset was converted to a 30-min flux dataset and added to the online data repository.

Soil heat flux (G) measurements were obtained using two sets of soil heat flux plates, a TCAV-averaging soil thermocouple and soil moisture probe (Campbell Scientific, Inc.) installed below the soil surface. Soil heat flux was measured by averaging measurements collected using HFP01 (Hukseflux, Inc.) and CN3 (Middleton Instruments) soil heat flux plates. Output voltage from heat flux plates was converted to soil heat flux using manufacturer-supplied calibration relationship.

3 | SOIL HYDROLOGICAL DATA

Soil moisture was measured using CS616 (Campbell Scientific, Inc.) water content reflectometers. Soil moisture probes consisted of two parallel stainless steel rods that measure dielectric permittivity of the surrounding medium. The CS616 sensor averaged water content over the entire length of the sensor. Soil moisture probes were installed vertically in the soil profile to measure soil moisture at 0–5, 0–30, 30–60, 60–90, and 90–120 cm. All probes were connected to a data logger that recorded the sensor output (wave period, mS) at 30-min intervals.

Soil moisture sensors typically require soil-specific calibration to provide accurate volumetric soil moisture measurements (Western et al., 2004). To undertake the calibration, undisturbed soil samples collected from the field sites in a metal tube were fully saturated in the laboratory. The saturated soil samples (with soil moisture sensors inserted) were placed in the temperature-controlled chamber for accelerated drying during which gravimetric soil moisture contents were measured for calibration. Similar approach had been used for the soil moisture sensor calibration (Rüdiger et al., 2010; Seyfried & Grant, 2007; Western & Seyfried, 2005).

The calibration coefficients were obtained from a curve fit of the laboratory period measurements and gravimetric measurements. The power function shown in Figure 4 indicates the best curve fit between period measurements and the gravimetric measurements with an R^2 value of .95 as shown in Figure 4. Different calibration relationships were obtained for different soil depths.

The in-field accuracy of CS616 soil moisture probes was checked by comparison with time domain reflectometer (TDR) measurements collected during our field visits. The root-mean-square difference between calibrated CS616 soil moisture measurements and TDR

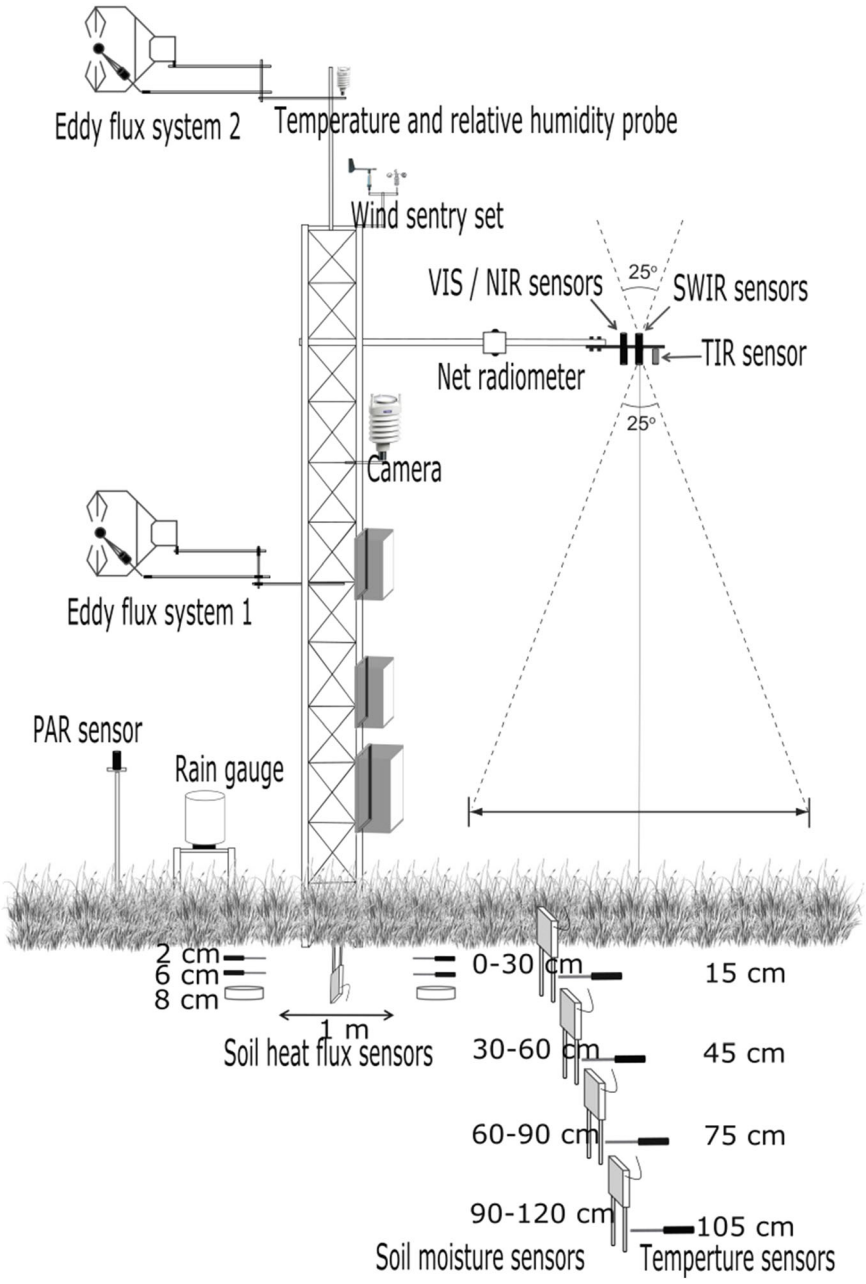

FIGURE 3 Schematic diagram of soil moisture and micrometeorological sensors installed at study sites

measurements was 4% v/v. The following equation shows conversion of 0- to 30-cm sensor outputs to volumetric soil moisture for Study Site 2.

$$SM_{0-30\ cm} = 0.000002^{*}\text{period}^{4.9276}. \quad (2)$$

4 | SPECTRAL DATA

4.1 | Surface reflectance

In this study, we used a ground-based system to monitor surface reflectance at both study sites. SKR-1850 and SKR-1870A light sensors (Skye Instruments Ltd, UK) installed at 5.7-m height were used to measure surface reflectance in six channels with wavelengths 527–537, 565–575, 620–670, 837–877, 1,228–1,248, and 2,110–2,148 nm. These systems were equipped with both upward- and downward-looking sensors to measure solar irradiance and canopy or soil reflectance, respectively. Sensors installed in study sites were used without the diffuser so that the output from each channel is sensitive to another channel. These data can be used to calculate vegetation indices such as NDVI and photochemical reflectance index.

The output from each channel records values in the form of current; the ratio sensitivity Z is introduced to convert the original equipment reading in nanoamps to $\mu mol \cdot s^{-1} \cdot m^{-2}$. Manufacturer-supplied relative sensitivity values were used to calculate reflectance for particular spectral bands. Using the measured spectral reflectance values, NDVI was calculated as follows:

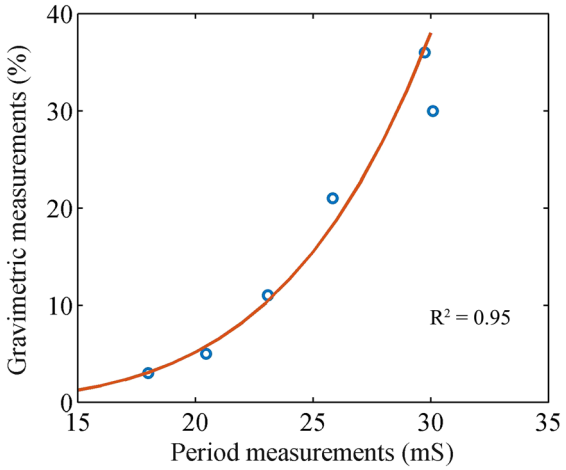

FIGURE 4 Scatter plot of period and gravimetric measurements for soil moisture 0–30 cm

$$NDVI = \frac{(Z^{*}NIR_{R(nA)}/X) - (Red_{R(nA)}/Y)}{(Z^{*}NIR_{R(nA)}/X) + (Red_{R(nA)}/Y)}, \quad (3)$$

where X is the NIR_I incident reading ($\mu mol \cdot s^{-1} \cdot m^{-2}$); Y is the Red_I incident reading ($\mu mol \cdot s^{-1} \cdot m^{-2}$); Z is the ratio sensitivity of reflected NIR:Red; $NIR_{R(nA)}$ is the reflected reading in nanoamps; and $Red_{R(nA)}$ is the reflected reading in nanoamps.

The output of each sensor was measured at 5-min intervals. Five-minute data were then converted to 30-min data by taking the average of six values. To better understand crop phenology, average midday NDVI values were produced for analysis. The NDVI dataset was smoothed by applying the Savitzky–Golay filter to reduce errors associated with unfavourable atmospheric conditions such as non-uniform cloud cover (Chen et al., 2004).

Ground-based NDVI measurements were evaluated against a time series of the MODIS 16-day composite of 250-m NDVI (MOD13Q1) product downloaded from the National Aeronautic and Space Administration (NASA) Land Process Distributed Active Archive Center (LPDAAC) (https://lpdaac.usgs.gov/lpdaac/get_data/data_pool) for the study area (Didan, 2015). The correlation between MODIS and ground-based NDVI values at Study Site 1 and Study Site 2 was 0.89 and 0.86 during the experimental period. The root-mean-square difference and bias were 0.11 and 0.06, respectively, at Site 1 and 0.17 and 0.08, respectively, at Site 2.

Spectral reflectances were also compared with CROPSCAN (MSR 16) measurements recorded during our field visits in the 2012 wheat crop season. CROPSCAN measurements were recorded at midday to minimize the effects of diurnal changes in solar zenith angle. The measurements were recorded near the footprint of the Skye sensors as well as at four other locations in the crop field. All reflectance measurements were averaged for each sampling location where five measurements were recorded at each location. The correlation between ground-based NDVI and average CROPSCAN NDVI measurements was 0.88.

Figure 5 shows time series of NDVI across three vegetation cycles. At Site 1, NDVI values were initially stable over time and then increased rapidly from February to March 2012 representing rapid lucerne growth following high rainfall. NDVI values decreased with sheep grazing activity in May 2012 and increased with of lucerne crop regrowth. Seasonal behaviour of the NDVI profile in 2013 and 2014 was due to seasonal variation in pasture and canola. Figure 5b shows analogous data for Study Site 2. NDVI fluctuations were clearly associated with two wheat crop seasons in 2012 and 2013 and the canola-cropping season in 2014. Fluctuations in NDVI values during August 2014 were related to yellow canola flowers present prior to seed formation.

4.2 | Radiative surface temperature

Ground-based radiative surface temperature was measured using an Apogee (SI-111) infrared radiometer. The sensor was equipped with a radiation shield and measured target thermal radiance in the 8- to 14-μm atmospheric window. This atmospheric window reduces the effects of water bands below 8 μm and above 14 μm. The sensor measured radiation emitted from the target, which was then converted to temperature using the Stefan–Boltzmann constant and an assumed surface emissivity of 1.0. Errors associated with sensor body temperature were corrected using manufacturer-supplied calibration coefficients. Radiative surface temperature was measured at 5-min intervals and then averaged to produce 30-min interval data (Figure 2c). Midday radiative surface temperature was compared with MODIS 8-day 1-km resolution temperature data (MOD11A2). The root-mean-squared error difference between ground-based radiative surface temperature and MODIS land surface temperature was 4.3°C.

5 | DATA QUALITY AND APPLICATIONS

5.1 | Data quality control

Data collected from experimental sites were visually inspected to identify errors. Errors associated with field activities were identified from daily photographs and removed from the dataset. Surface reflectance and radiative surface temperature data were compared with MODIS and CROPSCAN data. Variations in evapotranspiration were cross-checked with net radiation and air temperature. Errors or data gaps in meteorological data at one site were filled with meteorological data from the other site. Energy balance closure in the Study Sites 1 and 2 was 0.76 and 0.84, which indicates good energy budget closure during the study period.

Soil moisture data were checked by comparison with soil moisture from other layers and rainfall data. Soil moisture from 0 to 30 cm was also compared with TDR measurements collected during field visits. Rainfall data collected from tipping bucket rain gauges were shown to record more rainfall by a mean of 11% when compared with collecting rain gauge measurements recorded during field visits.

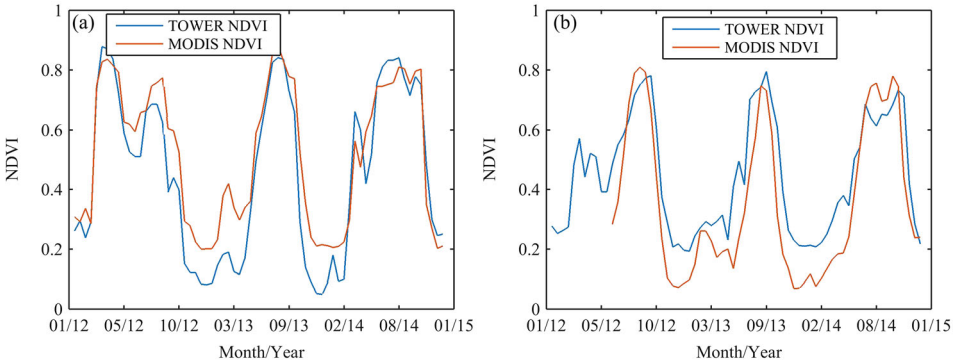

FIGURE 5 MODIS and TOWER normalized difference vegetation index (NDVI) time-series data at (a) Site 1 and (b) Site 2

5.2 | Applications

The Dookie hydrometeorological and spectral dataset can be used for various purposes. The dataset is useful for understanding the sensitivity of Evapotranspiration (ET) to root-zone soil moisture in agriculture landscapes (Akuraju, Ryu, George, Ryu, & Dassanayake, 2013, 2017) and how this relationship might manifest in remote sensing data. This dataset is also suitable for potential evapotranspiration calculations and land surface modelling. Surface reflectance data collected along with photos would be useful for understanding vegetation dynamics of different crops. Hydrometeorological and spectral datasets are well suited for validation and testing of remote sensing ET and Soil moisture (SM) products. Soil moisture data could be useful for developing models to estimate or validate surface and root-zone soil moisture based on optical and thermal remote sensing. Although the authors continue to analyse and utilize this dataset, it is available to other researchers to use.

5.3 | Data availability

The data that support the findings of this study are openly available in figshare at https://melbourne.figshare.com/projects/Dookie_hydrometeorological_dataset_2012-2014/61451. Data are shared under a Creative Commons attribution licence (CC BY) and must be appropriately cited.

6 | CONCLUSIONS

A comprehensive dataset including meteorological, soil moisture, surface flux, surface temperature, and spectral measurements over two rain-fed agricultural fields in Victoria, Australia, has been described. Data are available in 5- (spectral measurements) or 30-min resolutions over three growing seasons from 2012 to 2014. The data capture seasonal and shorter term variations in hydrometeorological and reflectance conditions of the sites. Comparison with MODIS remote sensing products shows a high correlation over time. The data are useful for a wide range of land surface research purposes and are openly available to users.

ACKNOWLEDGMENTS

This research was funded in part by The Australian Research Council—Linkage Infrastructure, Equipment and Facilities (ARC-LIEF) Grant LE130100040. The authors would also like to thank the Australian Centre for International Agricultural Research (ACIAR) for sponsoring this research under the John Allwright Fellowship. The authors are grateful to Robert Pipunic, Kithsiri Dassanayake, Aishwarya Kunnath Poovakka, and Minoo Hashemian Rahaghi for their support in field activities and data processing.

CONFLICT OF INTERESTS

The authors declare that there is no conflict of interest regarding the publication of this paper.

ORCID

Venkata Radha Akuraju https://orcid.org/0000-0002-7022-8444

REFERENCES

Akuraju, V. R., Ryu, D., George, B., Ryu, Y., & Dassanayake, K. (2013). Analysis of root-zone soil moisture control on evapotranspiration in two agriculture fields in Australia. In J. Piantadosi, R. S. Anderssen, & J. Boland (Eds.), *MODSIM2013, 20th International Congress on Modelling and Simulation*. Adelaide: Modelling and Simulation Society of Australia and New Zealand.

Akuraju, V. R., Ryu, D., George, B., Ryu, Y., & Dassanayake, K. (2017). Seasonal and inter-annual variability of soil moisture stress function in dryland wheat field, Australia. *Agricultural and Forest Meteorology*, *232*, 489–499. https://doi.org/10.1016/j.agrformet.2016.10.007

Bell, M. J., Eckard, R. J., & Cullen, B. R. (2012). The effect of future climate scenarios on the balance between productivity and greenhouse gas emissions from sheep grazing systems. *Livestock Science*, *147*(1–3), 126–138. https://doi.org/10.1016/j.livsci.2012.04.012

Chen, J., Jönsson, P., Tamura, M., Gu, Z., Matsushita, B., & Eklundh, L. (2004). A simple method for reconstructing a high-quality NDVI time-series data set based on the Savitzky–Golay filter. *Remote Sensing of Environment*, *91*(3–4), 332–344. https://doi.org/10.1016/j.rse.2004.03.014

Didan, K. (2015). MOD13Q1 MODIS/Terra Vegetation Indices 16-Day L3 Global 250m SIN Grid V006 [Data set]. NASA EOSDIS LP DAAC. DOI: https://doi.org/10.5067/MODIS/MOD13Q1.006

Moncrieff, J. B., Massheder, J. M., de Bruin, H., Elbers, J., Friborg, T., Heusinkveld, B., … Verhoef, A. (1997). A system to measure surface

fluxes of momentum, sensible heat, water vapour and carbon dioxide. *Journal of Hydrology*, *188–189*, 589–611. https://doi.org/10.1016/S0022-1694(96)03194-0

Rüdiger, C., Western, A. W., Walker, J. P., Smith, A. B., Kalma, J. D., & Willgoose, G. R. (2010). Towards a general equation for frequency domain reflectometers. *Journal of Hydrology*, *383*(3), 319–329. https://doi.org/10.1016/j.jhydrol.2009.12.046

Seyfried, M. S., & Grant, L. E. (2007). Temperature effects on soil dielectric properties measured at 50 MHz. *Vadose Zone Journal*, *6*(4). https://doi.org/10.2136/vzj2006.0188

Webb, E. K., Pearman, G. I., & Leuning, R. (1980). Correction of flux measurements for density effects due to heat and water vapour transfer. *Quarterly Journal of the Royal Meteorological Society*, *106*(447), 85–100. https://doi.org/10.1002/qj.49710644707

Western, A. W., & Seyfried, M. S. (2005). A calibration and temperature correction procedure for the water-content reflectometer. *Hydrological Processes*, *19*(18), 3785–3793. https://doi.org/10.1002/hyp.6069

Western, A. W., Zhou, S.-L., Grayson, R. B., McMahon, T. A., Blöschl, G., & Wilson, D. J. (2004). Spatial correlation of soil moisture in small catchments and its relationship to dominant spatial hydrological processes. *Journal of Hydrology*, *286*(1–4), 113–134. https://doi.org/10.1016/j.jhydrol.2003.09.014

How to cite this article: Akuraju VR, Ryu D, Western AW, Ian Young R. Towards estimating root-zone soil moisture using surface multispectral and thermal sensing: A spectral and hydrometeorological dataset from the Dookie experiment site, Victoria, Australia. *Hydrological Processes*. 2019;1–7. https://doi.org/10.1002/hyp.13459